Calculation of the Point Spread Function for the X09DA Pinholes in SLS

Natalia Milas, Angela Saa Hernandez

Paul Scherrer Institut, CH-5232 Villigen PSI, Switzerland

The diagnostic beamline X09DA is equipped with a set of x-ray pinholes for horizontal beam size measurements. In order to extract the right beam size out of the pinhole images it is necessary to carefully account all the effects that can add up to the image blurring. This is done by calculating the point spread function (PSF) of the system, which is a weighted average over the x-ray spectra of the blurring effects of diffraction, pinhole geometry, scintillator and CCD camera. In this note we describe, step-by-step, the details of this calculation.

1   Introduction

The SLS is a 3rd generation light source that delivers to its users high brightness synchrotron radiation. The stored electron energy is 2.4 GeV and the total current 400 mA. Like other 3rd generation light sources SLS is able to operate at very low coupling, close to 0.01%. Measurements of the transverse beam size, and inference of the transverse emittance and local coupling, can be done at the dedicated beamline X09DA. The radiation of the source dipole is simultaneously used on two different branches of the beamline for beam size diagnostics. On one branch x-rays are used for pinhole imaging, while on the other branch vertically polarised visible/UV light is imaged following the π-polarisation method [1]. For the accurate measurement of very small vertical beam sizes the π-polarisation method has to be used due to its higher resolution. Instead, for the accurate measurement of the horizontal beam size the preferred option is the imaging with a set of pinholes of different sizes.

The use of x-ray pinholes for beam size measurements is specially important during some special shifts at SLS, aimed to study intra-beam scattering (IBS) effects. On those shifts the machine runs at a lower energy (1.6 GeV) and the variations of the horizontal beam size as a function of current are expected to be on the order of 10% [2], for which a highly sensitive diagnostic system and data analysis is essential.

To calculate the horizontal beam size the point spread function (PSF) of the system has to be deconvoluted from the measurements at the CCD camera. In this note the calculation of the PSF is explained step-by-step, taking into account the broadband spectrum of the bending magnet source.

2   The x-ray branch

The layout of the x-ray branch of beamline X09DA is sketched in figure 1 (top). The source of the synchrotron radiation (SR) is the central dipole of sector 9, BX09. A water cooled pinhole array, fabricated from a 150 μm Tungsten sheet, is situated at 4.093 m from the dipole center. The pinholes of 15, 20, 25 and 30 μm aperture diameter are arranged in a total of eight columns, two of each size, as plotted in figure 2. The light escaping these holes travels along the beamline and exits through a vacuum window. At the end of the beamline, outside the vacuum, an optical table is placed. On top of the optical table there is a movable Molybdenum attenuator, consisting of 5 Mo foils of 40 μm each. One can decide how many foils are placed on the beam path to attenuate the transmission and filter the bandwidth. Right after the Mo attenuator a P43 phosphor screen is used to convert the x-rays in visible light centered around 550 nm (green). The phosphor screen is also called the scintillator screen. The visible light is zoomed and focused with an adjustable lens system into a CCD camera with a pixel size of 4.65 $\times$ 4.65 μm.
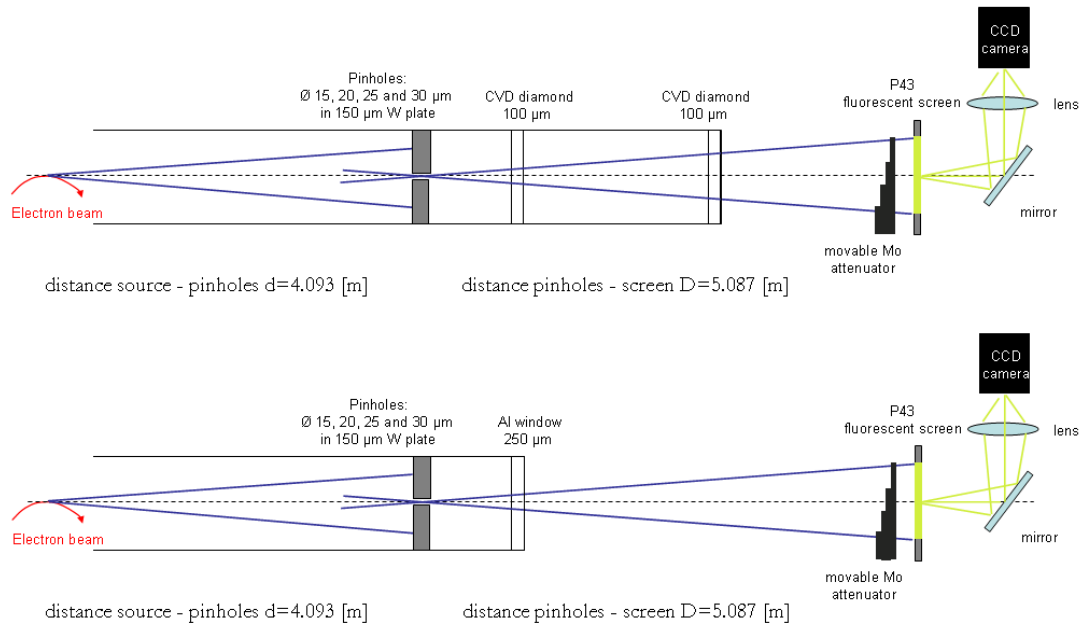
Figure 1: Current layout of the x-ray branch (top). Previous layout of the x-ray branch of the X09DA beamline (bottom).

2.1 Beamline upgrades for the IBS measurements

From 2006, when the beamline was built, and until October 2012, when the beamline was upgraded to adapt it to the IBS shifts, not much had been changed since the visible/UV branch was the one mostly used for beam size measurements during users' shifts. This scenario changed once we started a set of experiments for the TIARA project [3], trying to measure IBS growth in SLS while running the machine at lower energy.

The main upgrade was to replace the beamline exit window, made of a 250 μm thick Aluminium disc by a 100 μm thick CVD diamond window, which allows a higher x-ray transmission. Due to the small size of the CVD diamond window, 11×40 mm (width×height), it is bonded in the center of a stainless steel flange. As the beamline is directly connected to the ring vacuum and there is no fast valve protection, a 100 μm kapton foil was included upstream the window to avoid the risk of leakage in the bonding. But the x-rays burned the kapton foil in less than a week and the same occurred using a thicker (120 μm) kapton foil. Finally two CVD diamond windows were used, separated approximately 3 m, being the outer one only 0.5 m away from the screen. Due to the small size of these windows and the long distance from the second one to the x-ray source, only the light of 3×3 pinholes exits the windows and can be imaged (2×15 μm and 1×20 μm), while the light from the other pinholes is cut by the window's physical aperture. A sketch of the initial layout of the x-ray branch of beamline X09DA is represented in figure 1 (bottom).
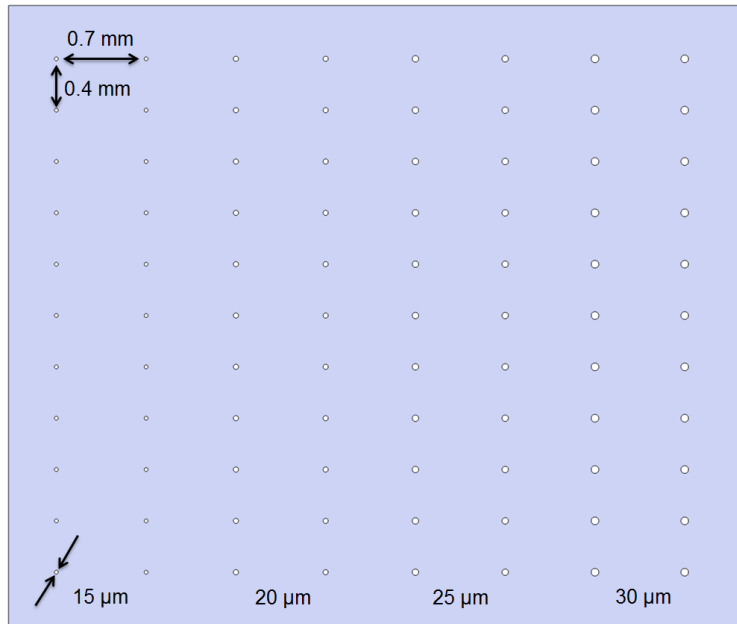
Figure 2: Pinhole array.

2.2 Transmission intensity

The transmittance, as a function of the photon energy, of the different materials in the light path have to be taken into account to estimate the spectral distribution of the SR reaching the phosphor screen. In figure 3 (top) the transmittances through the different window materials and along the beam path in air are plotted. In figure 3 (bottom) are represented the transmittances of the different possible combinations of the Molybdenum sheets. The combined effects of the windows and the Molybdenum filters on the light transmission are shown in figure 4 for both energies of the electron beam; 1.6 and 2.4 GeV. For IBS studies, at 1.6 GeV, no Molybdenum filter should be used, since the intensity of the transmitted light reaching the CCD camera is very low.

4
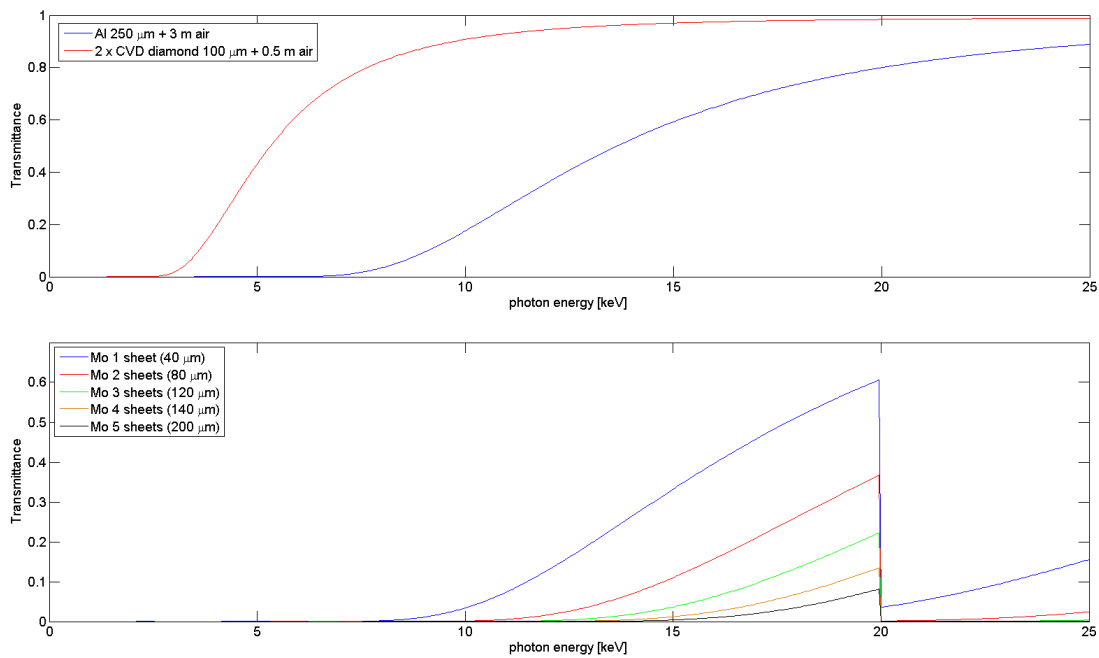
Figure 3: Transmittance through the different window materials and along the beam path in air (top). Transmittance through the Mo filters (bottom).
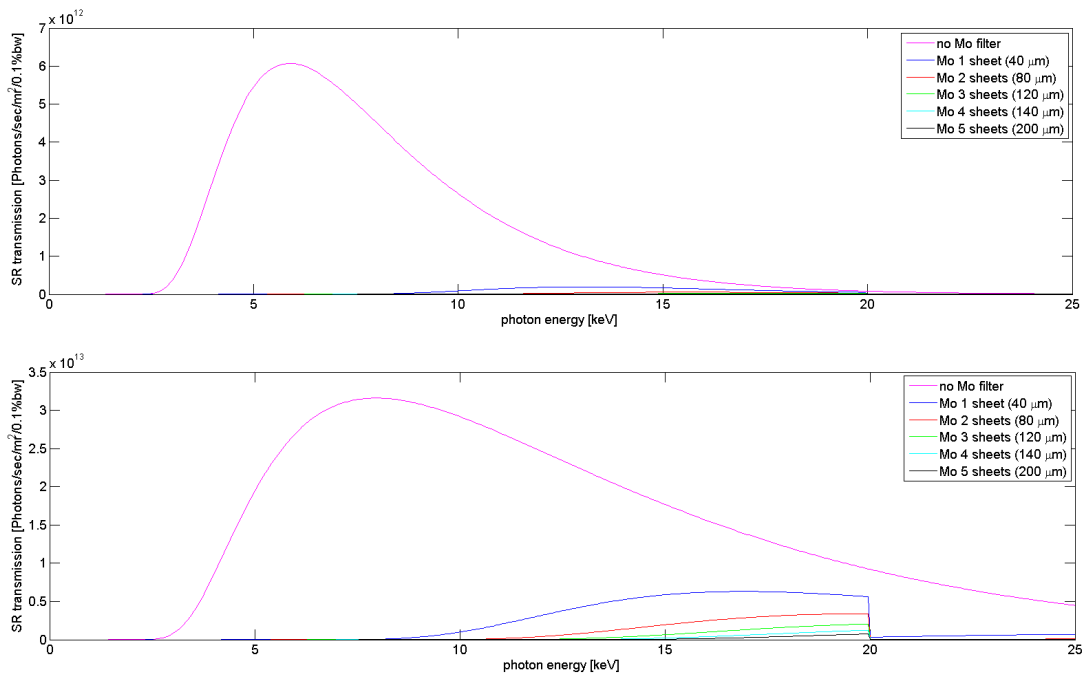
Figure 4: Transmission of SR through the CVD diamond windows and the Mo filters for the low energy mode (1.6 GeV) of the machine (top), and for the standard energy mode (2.4 Gev) (bottom).

3 Point Spread Function calculation

The image formed on the camera is the convolution of the source profile and the PSF of the imaging system. In order to clear out the size of the SR source the image has to be deconvolved with the PSF of the imaging system. We assume the resolution limit of the pinholes to be given by the corresponding PSF, as the measurement of source sizes smaller than the PSF, though possible, is very prone to errors.

To analytically calculate the PSF of the system we will, in a first approximation, assume to be in the far-field region, also called Fraunhofer region. This is true when the distance between the pinhole and the screen in which the light is observed is significantly greater than A^2/λ, where λ is the wavelength and A is the pinhole diameter. This condition is not fulfilled by all our pinhole apertures, specially by the larger ones, but still we consider that the model provides a clear and intuitive treatment of the problem that is worth to be presented. The results from this inaccurate analytical model will later be compared to some results obtained from a numerical calculation. Only in the far-field region the calculation of the diffraction can be simplified by using the Fraunhofer diffraction equation, and the resulting PSF can be approximated to a Gaussian function. The rms of the Gaussian fit (i.e. the σ) of the image on the camera is defined as Σ and fulfills:

$$\Sigma^2 = S^2 + \Sigma_0^2 \tag{1}$$

where Σ_0 is the σ of the PSF and S is the σ of the source.
Following the approach from [5], the PSF of the system can be decomposed into 2 contributions; the contribution from the pinholes $S_{pinhole}$ and the contribution from the imaging system (phosphor screen and CCD camera) S_{camera}, which add up quadratically:

$$\Sigma_0^2 = S_{pinhole}^2 + S_{camera}^2 \tag{2}$$

3.1 Pinholes

The pinhole contribution to the PSF can be further decomposed into 2 contributions: $S_{aperture}$ and S_{diff}. $S_{aperture}$ is the geometrical projection of the pinhole opening. A point source of light illuminating a hole at a distance d, will project a spot of light on the scintillator screen. The size of this spot is $A(D + d)/d$, where A is the pinhole diameter and D is the distance from the pinhole to the screen. The camera geometric magnification is D/d, and the corresponding σ of this contribution to the total measured beam size is:

$$S_{aperture} = \frac{A}{\sqrt{12}} \frac{D + d}{D} \tag{3}$$

where the factor $\sqrt{12}$ is due to the conversion of the width of the rectangular profile to an rms value.
S_{diff} accounts for the pinhole diffraction, which in the regime of Fraunhofer diffraction is described by a Bessel function of first order, for a circular pinhole. If the Bessel

function of first order is approximated by a gaussian function, the σ of the diffraction contribution to the total beam size is:

$$S_{diff} = 0.42\frac{\lambda D}{A} \tag{4}$$

Thus, pinholes with large apertures will lead to image blurring due to geometrical shadowing while pinholes with small apertures have strong diffraction effects. The total contribution from the pinholes to the PSF, as a function of the photon energy for the different pinhole apertures, is shown in figure 5.
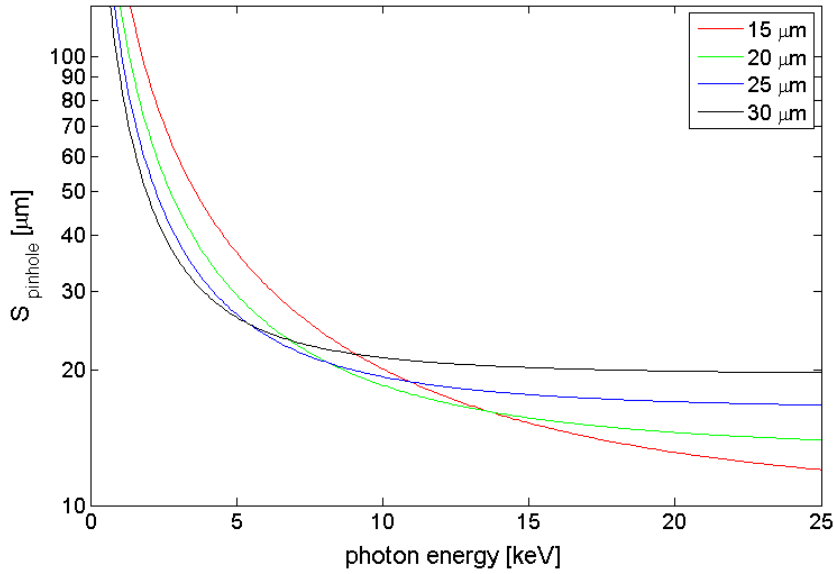
Figure 5: Point spread function of the system due to the pinholes calculated analytically for the different pinhole diameters.

However, in the case of the pinholes of SLS the far-field region condition is not fulfilled in some cases. Thus, the expressions given above assuming gaussian functions are not valid in those cases. An example is shown in figure 6 where it can be observed that for a photon energy of 20 keV the diffraction pattern from the the larger pinholes is very far from a gaussian function. In order to account for the near-field diffraction effects which were neglected by the Fraunhofer equation we used, the PSF has been numerically calculated as a function of the photon energy for each pinhole size using the Synchrotron Radiation Workshop (SRW) program [4]. The results are shown in figure 7, compared to those from the analytical calculations. A similar discrepancy between the analytical calculations assuming a far-field approximation and the numerical calculations done with SRW was already found at SOLEIL [6].

With the knowledge of the x-ray transmission along the beamline and the pinhole PSF values from figure 7 it is possible to account for the non monochromatic x-ray

Table 1: PSF of the pinholes for the standard energy (2.4 GeV).

Pinhole size [μm]	$S_{pinhole}$ [μm]					
	no Mo	1 Mo foil	2 Mo foils	3 Mo foils	4 Mo foils	5 Mo foils
15	16.9	10.0	8.9	8.5	8.1	7.6
20	12.7	7.6	6.8	6.5	6.2	5.8
25	10.2	6.3	6.0	6.0	6.0	5.8
30	8.7	7.7	11.0	13.3	14.4	14.6

Table 2: PSF of the pinholes for the low energy mode (1.6 GeV).

Pinhole size [μm]	$S_{pinhole}$ [μm]					
	no Mo	1 Mo foil	2 Mo foils	3 Mo foils	4 Mo foils	5 Mo foils
15	21.1	9.2	7.7	6.9	6.5	6.3
20	16.0	7.0	6.0	5.3	5.1	5.0
25	12.8	6.3	5.8	5.4	5.2	5.2
30	10.4	13.2	14.0	13.6	13.5	13.4

spectrum. Tables 1 and 2 show the calculated pinhole PSF integrated over the spectrum for all pinhole sizes, for the standard and low energy modes of SLS, respectively.

3.2 Phosphor screen and camera set

The contribution of the imaging system to the PSF can be further decomposed into 2 contributions: S_{screen} and S_{CCD}. These terms add up quadratically fulfilling:

$$S^2_{camera} = S^2_{screen} + S^2_{CCD} \tag{5}$$

S_{screen} accounts for the blurring of the final image due to the thickness and grain size of the phosphor screen. We approximate the blurring caused by thickness of the phosphor screen to the value of its thickness, which can be of 6 μm or 10 μm. Currently a 10 μm thick screen is installed. The grain size of the phosphor screen is 2 to 3 μm. To calculate the effect of the grain size on the image we convolute the image at the screen with the grain size. The image at the screen can be approximated by a gaussian function with $\sigma = 75\mu$m, equal to the product of the the magnification of the beamline, M=1.24, with the horizontal size of the electron beam, which is also approximated by a gaussian function with $\sigma = 60\mu$m. The convolution of the image at the screen with a rectangular function with a 3 μm width results in a gaussian curve with a $\sigma = 75.05\mu$m. That is, the distortion of the image in the screen is less than 1/1000, which we consider negligible.

S_{CCD} is the spatial resolution of the camera. Knowing that the pixel size of the CCD

camera is 4.65 $\times$ 4.65 μm and the magnification of the whole beam line is M=1.24, we can calculate the resolution given by the CCD to be the ratio between the pixel size and M, thus S_{CCD}= 3.75 μm.

The resulting PSF of the imaging system has a value of 7.1 μm if a 6 μm thick phosphor screen is used, and a value of 10.7 μm if a 10 μm thick phosphor screen is used.

3.3   PSF results

The PSF of the imaging system (Σ_0), calculated taking into account the contributions of the pinholes, phosphor screen and CCD camera, are presented in tables 3, 4, 5, and 6, for the standard and low energy modes of SLS, and for different beamline settings (see specifications in table captions). The optimum conditions are different for measurements at 2.4 and 1.6 GeV, since a different part of the x-ray spectrum is used. For the 2.4 GeV the optimum setup is to use the 20 μm or the 25 μm pinholes set, with all or almost all Mo filter sheets. Instead, for 1.6 GeV the 30 μm ones are more fit if no Mo filter is used. Anyhow, it has to be noticed that the PSF decreases dramatically, thus increasing the resolution limit, if one or more Mo filter sheets are used. The only reason for which they cannot be used in this case is that not enough light is detected by the camera. This situation could probably be changed with the installation of a more sensitive camera. In that case, one or more Mo filters could be used and the optimum pinholes would be those of 20 or 25 μm. With the beamline upgrades, however, we cannot detect light from the 25 μm and 30 μm pinholes any longer and in such case the 20 μm pinholes are the best solution for both operating energies.

Table 3: PSF of the full imaging system for the standard energy with a 6 μm P43 screen.

Pinhole size [μm]	Σ_0 [μm]					
	no Mo	1 Mo foil	2 Mo foils	3 Mo foils	4 Mo foils	5 Mo foils
15	18.3	12.3	11.4	11.1	10.7	10.4
20	14.6	10.4	9.9	9.6	9.5	9.2
25	12.4	9.5	9.3	9.3	9.3	9.2
30	11.3	10.5	13.1	15.1	16.1	16.2

Table 4: PSF of the full imaging system for the standard energy with a 10 μm P43 screen.

Pinhole size [μm]	Σ_0 [μm]					
	no Mo	1 Mo foil	2 Mo foils	3 Mo foils	4 Mo foils	5 Mo foils
15	20.0	14.6	13.9	13.7	13.4	13.1
20	16.6	13.1	12.7	12.5	12.4	12.2
25	14.8	12.4	12.2	12.3	12.3	12.2
30	13.8	13.2	15.3	17.1	18.0	18.1

Table 5: PSF of the full imaging system for the low energy mode with a 6 μm P43 screen.

Pinhole size [μm]	Σ_0 [μm]					
	no Mo	1 Mo foil	2 Mo foils	3 Mo foils	4 Mo foils	5 Mo foils
15	22.2	11.6	10.5	9.9	9.6	9.5
20	17.5	10.0	9.3	8.9	8.7	8.6
25	14.6	9.5	9.1	8.9	8.8	8.8
30	12.6	14.9	15.7	15.4	15.2	15.2

Table 6: PSF of the full imaging system for the low energy mode with a 10 μm P43 screen.

Pinhole size [μm]	Σ_0 [μm]					
	no Mo	1 Mo foil	2 Mo foils	3 Mo foils	4 Mo foils	5 Mo foils
15	23.6	14.1	13.2	12.7	12.5	12.4
20	19.2	12.8	12.3	12.0	11.8	11.8
25	16.7	12.4	12.1	12.0	11.9	11.9
30	14.9	17.0	17.6	17.3	17.2	17.2
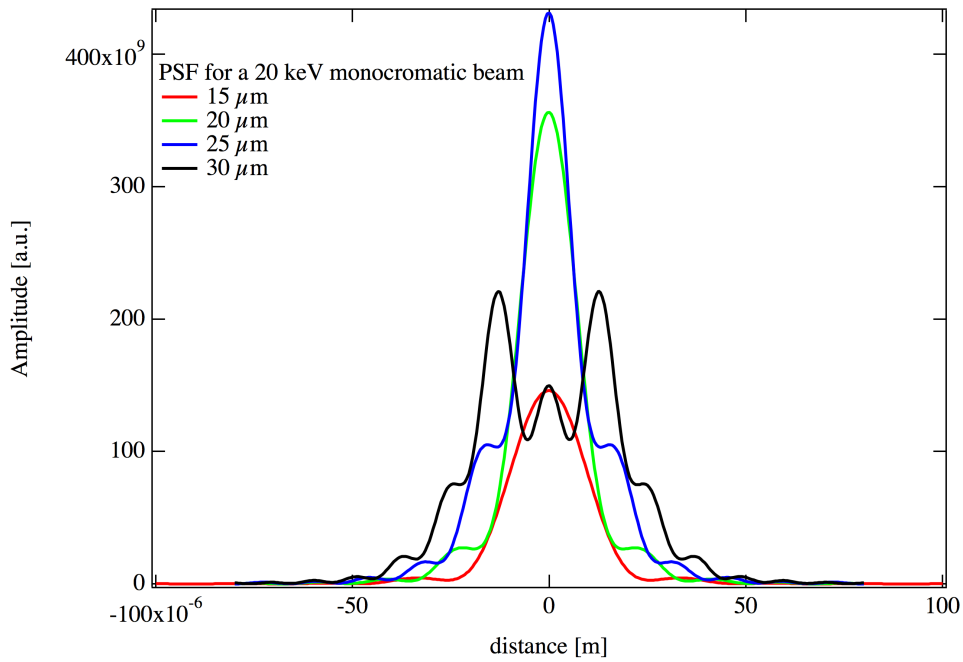
Figure 6: Point spread function of the system for 20keV.
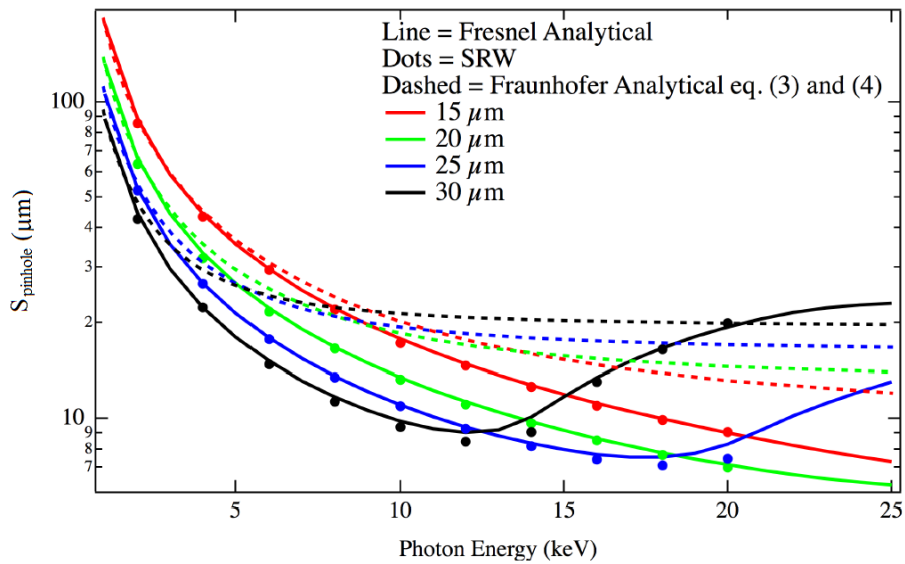
Figure 7: Point spread function of the system numerically calculated with SRW for the different pinhole diameters (dots) and the analytical results using Fraunhofer approximation like described in equations (3) and (4) (dashed line) and Fresnel approximation (full lines).

4 New Matlab GUI

In order to have a measurement application with the ability to save pinhole images for post processing a simple MATLAB GUI was developed. Figure 8 shows how the GUI looks like for the end user. One of the main features of this GUI is that the user can save automatically (button "Save Image(s)") a set of pictures of the pinholes with a set of information like the size of the pinhole used, the exposure time, etc. It is also possible to save and subtract a background image and specify a region of interest (ROI). Using the "Do Fit" button a 2D-Gaussian is fitted to the image. At all times the vertical and horizontal profiles are shown together with the image. When using the "Img. Loop" button a third plot with the values of the horizontal and vertical rms width of the image can be plotted. On the right top corner the maximum pixel value is used to warn the user when getting into saturation regime. With the GUI it is also possible to load (button "Load Image") previously saved images for post processing.
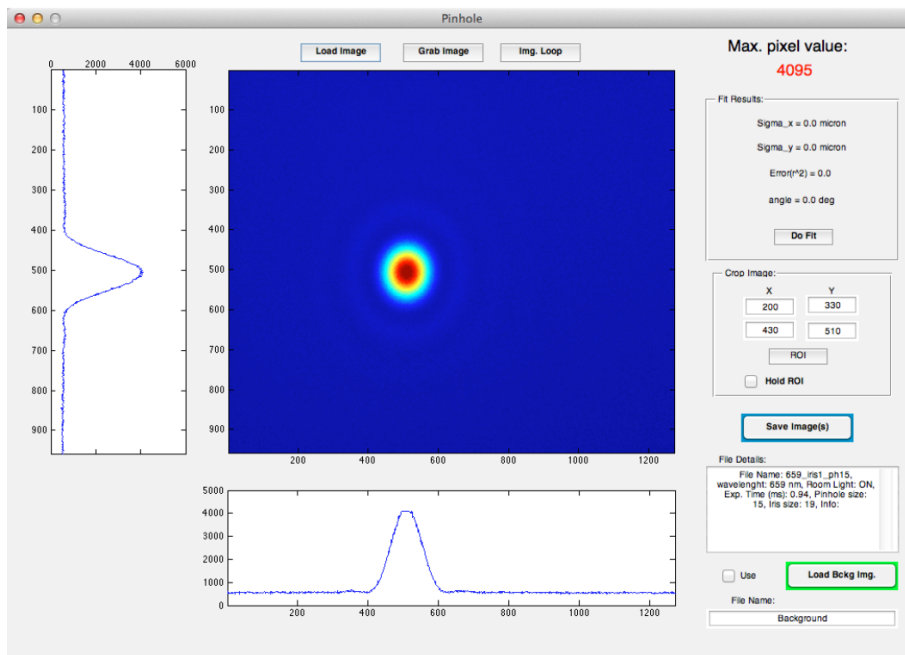
Figure 8: Window of the MATLAB GUI.

12

References

[1] Å. Andersson et al., Nucl. Instrum. Methods Phys. Res., Sect. A 591 (2008) 437-446.

[2] F. Antoniou et al. "Optics design optimization for IBS dominated beams", WEO1B02, High-Intensity and High-Brightness Hadron Beams 2012, Beijing, China.

[3] TIARA WP6: SVET R&D infrastructure, `http://www.eu-tiara.eu/rtd/index.php?id=42`, 2011.

[4] O. Chubar, P. Elleaume, "Accurate and efficient computation of synchrotron radiation in the near field region", EPAC'98, Stockholm 1998, THP01G, p. 1177.

[5] C. Thomas et al. "X-ray pinhole camera resolution and emittance measurement", PRST-Accelerators and beams 13, 022805 (2010).

[6] M.-A. Tordeux et al. "Ultimate resolution of SOLEIL x-ray pinhole camera", DIPAC'07, Venice 2007, TUPC16.